

## Synthesis and Improved Properties of Nanostructured $\text{Li}_2\text{MnSiO}_4/\text{C}$ via a Modified Sol-gel Method

C. Deng<sup>1,\*</sup>, Y. H. Sun<sup>1</sup>, S. Zhang<sup>2,\*</sup>, H. M. Lin<sup>1</sup>, Y. Gao<sup>1</sup>, B. Wu<sup>1</sup>, L. Ma<sup>1</sup>, Y. Shang<sup>1</sup>, G. Dong<sup>1</sup>

<sup>1</sup> Key Laboratory of Design and Synthesis of Functional Materials and Green Catalysis, Colleges of Heilongjiang Province; College of Chemistry and Chemical Engineering, Harbin Normal University, Harbin, 150025, Heilongjiang, China

<sup>2</sup> College of Material Science and Chemical Engineering, Harbin Engineering University, Harbin 150001, Heilongjiang, China

\*E-mail: [chaodeng2008@yahoo.cn](mailto:chaodeng2008@yahoo.cn); [senzhang@hrbeu.edu.cn](mailto:senzhang@hrbeu.edu.cn)

Received: 12 March 2012 / Accepted: 4 April 2012 / Published: 1 May 2012

---

Nanostructured  $\text{Li}_2\text{MnSiO}_4/\text{C}$  was synthesized by a modified sol-gel method. X-ray diffraction pattern confirms the formation of orthorhombic structure with group space  $Pmn2_1$ . SEM and TEM observations show nanostructured particles of about 80 nm and a thin surface layer of residual carbon. Raman analysis reveals the carbon is mainly amorphous. Electrochemical testing results indicate improved charge/discharge capacities and cycling performance of  $\text{Li}_2\text{MnSiO}_4/\text{C}$  compared with the pristine  $\text{Li}_2\text{MnSiO}_4$ . Indicated by EIS results,  $\text{Li}_2\text{MnSiO}_4/\text{C}$  has smaller charge transfer resistance than the pristine  $\text{Li}_2\text{MnSiO}_4$ , which suggests its enhanced conductivity and results in the improved electrochemical properties.

---

**Keywords:**  $\text{Li}_2\text{MnSiO}_4/\text{C}$ ; nanoparticle; carbon coating; electrochemical property

### 1. INTRODUCTION

Lithium transition-metal silicates with the general formula  $\text{Li}_2\text{MSiO}_4$  (M = Fe, Mn, Co, Ni) is attractive as positive electrode for lithium ion battery due to its improved safety and high theoretical capacity. Among the  $\text{Li}_2\text{MSiO}_4$  family,  $\text{Li}_2\text{FeSiO}_4$  and  $\text{Li}_2\text{MnSiO}_4$  are two important members which have attracted intensive attention [1-4]. Nyten et al firstly reports the synthesis of  $\text{Li}_2\text{FeSiO}_4$ . It exhibits a stable cycle life with a reversible capacity of around 160 mAh  $\text{g}^{-1}$  [5]. Compared with  $\text{Li}_2\text{FeSiO}_4$ ,  $\text{Li}_2\text{MnSiO}_4$  has a higher theoretical capacity and cell voltage based on the two electrons redox couples ( $\text{Mn}^{2+/3+}$  and  $\text{Mn}^{3+/4+}$ ), which makes it a more promising cathode candidate [6-8].

However, the major drawback of the orthosilicates is their low electronic conductivity and poor ionic mobility [9]. The inherent conducting properties greatly affect their electrochemical performance and inhibit the further use in commercial applications. To overcome this obstacle, the modification strategies such as the conductive carbon coating [10], the particle size reduction [11], and the cations doping [12] have been applied on the orthosilicates. Among these strategies, reducing the particle size is an effective way to increase the surface area and decrease the diffusion distance for charge transfer. Therefore, various solution-based synthesis methods such as sol-gel, combustion, hydrothermal, reflux have been pursued to obtain nanoparticles of  $\text{Li}_2\text{MnSiO}_4$ . R. Dominko et al [13] synthesized  $\text{Li}_2\text{MnSiO}_4$  particles of about 70 nm via a modified Pechini sol-gel method. In previous study, we also reported the preparation of nanoparticles for  $\text{Li}_2\text{MnSiO}_4$  by a citric acid assisted sol-gel method [14].

Although the solution-based synthesis successfully produce  $\text{Li}_2\text{MnSiO}_4$  nanoparticles, the phase structure and the electrochemical performance of the prepared materials are not satisfactory. It is still challenge to obtaining a phase pure material with desired particle size and good electrochemical characteristics by these methods. In order to improve the properties of lithium manganese orthosilicate, the nanostructured  $\text{Li}_2\text{MnSiO}_4$  with carbon coating layer was synthesized via a modified sol-gel method. The prepared  $\text{Li}_2\text{MnSiO}_4/\text{C}$  material exhibits nanometer size particles and improved electrochemical characteristics. The physical and chemical characteristics of the prepared  $\text{Li}_2\text{MnSiO}_4/\text{C}$  were investigated in detail.

## 2. EXPERIMENTAL

The  $\text{Li}_2\text{MnSiO}_4$  was prepared by a modified sol-gel method. A water-ethanol solution of tetraethyl orthosilicate (TEOS) was mixed with stoichiometric amount of lithium acetate and manganese acetate. Then the mixture was transferred into a reflux system where the acetic acid solution was added as a catalyst. The reflux was carried out under magnetic stirring at 80 °C for 20 h. The solution was then heated at 80 °C under magnetic stirring to evaporate the solvents gradually. After the solvents were evaporated, the resulting dry gel was grounded and calcinated at 650°C for 10h in flowing argon. Then the prepared  $\text{Li}_2\text{MnSiO}_4$  was mixed with desired amount of sucrose and the mixture was calcinated at 650 °C for 2h in flowing argon to synthesize the  $\text{Li}_2\text{MnSiO}_4/\text{C}$  material.

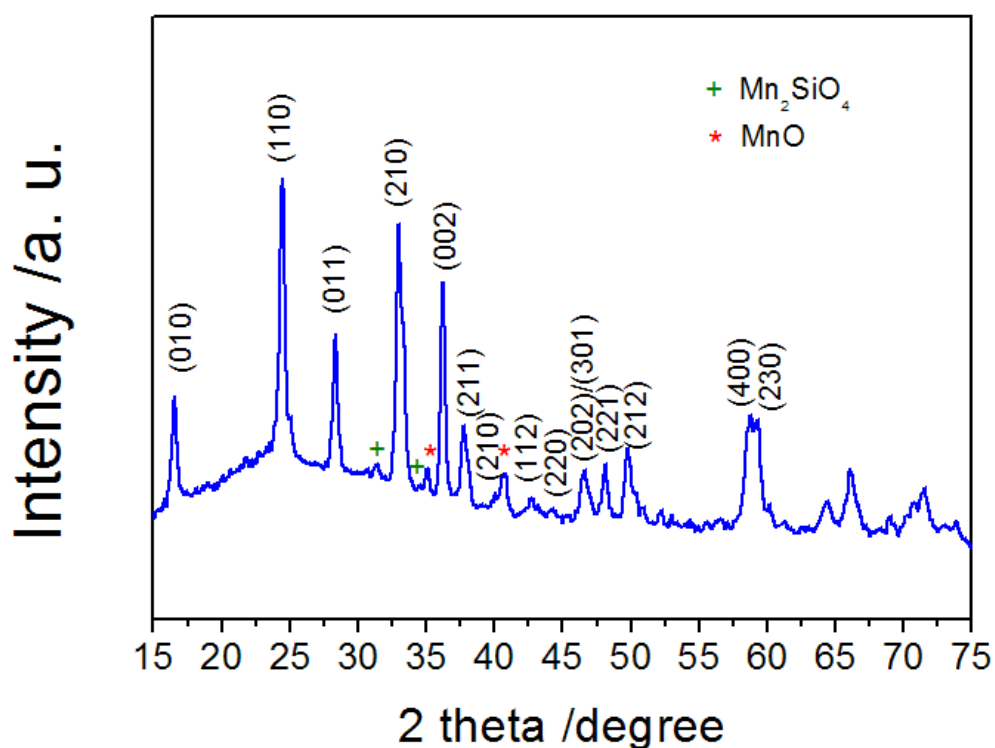
Powder X-ray diffraction (XRD, Bruker D8/Germany) employing Cu  $K\alpha$  radiation was used to identify the crystalline phase of the samples. The morphology was observed with a field emission scanning electron microscope (SEM, HITACHI S-4800) coupled with an energy dispersive X-ray detector (EDX). The surface of the sample was observed with a transmission electron microscopy (TEM, JEOS-2010 PHILIPS). The carbon content was determined by thermogravimetric analysis (TGA, Pyris Diamond PE).

The coin cells were prepared as described in Ref. [15]. The composite electrode was made from a mixture of the active material, acetylene black, and Polyvinylidene Fluoride in a weight ratio of 80:10:10. The 1 mol·L<sup>-1</sup>  $\text{LiPF}_6$  dissolved in a mixture of ethylene carbonate (EC) and diethyl carbonate (DMC) was used as the electrolyte. Galvanostatic charge-discharge measurements were performed in a

potential range of 1.5-4.6 V at ambient temperature. The electrochemical impedance measurements were carried out with a CHI 660 C instrument.

### 3. RESULTS AND DISCUSSION

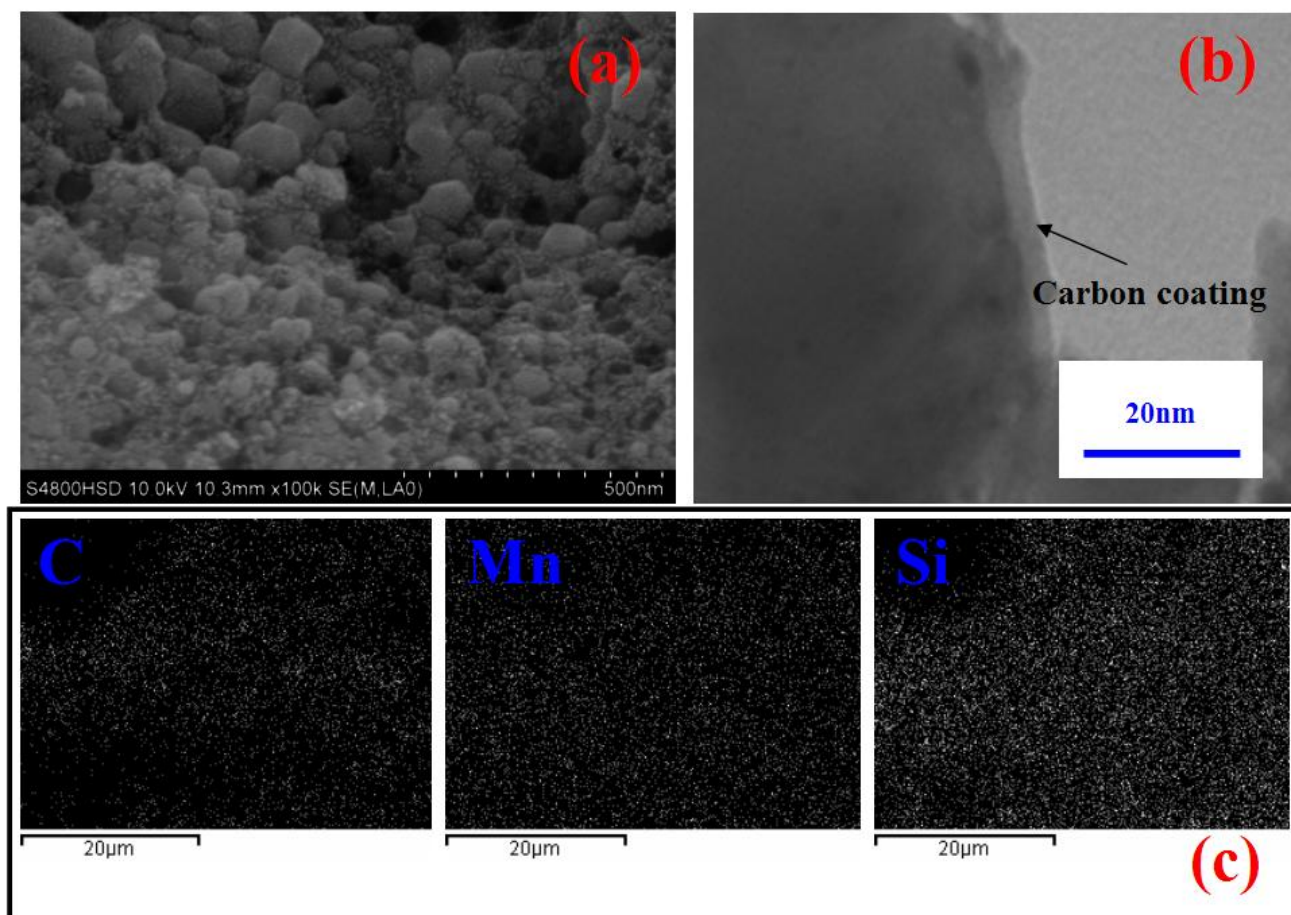
The XRD of the  $\text{Li}_2\text{MnSiO}_4/\text{C}$  sample is shown in Figure 1. The main peaks can be indexed on the basis of the orthorhombic unit cell in space group  $Pmn2_1$ . The  $\text{Li}_2\text{MnSiO}_4$  can be isostructural to certain forms of  $\text{Li}_3\text{PO}_4$  [16].  $\text{Mn}^{2+}$  ions are present within a  $[\text{SiO}_4]$  anionic silicate network that replaces  $[\text{PO}_4]$  anionic phosphate network, and two lithium ions are available in 3D dimensional channels [17]. However, a small amount of impurities of  $\text{MnO}$  and  $\text{Mn}_2\text{SiO}_4$  are observed in the samples. Many researchers have reported the presence of similar kinds of impurities in the  $\text{Li}_2\text{MnSiO}_4$  samples prepared by various methods [13,14,18,19]. In fact, the preparation of phase-pure  $\text{Li}_2\text{MnSiO}_4$  is very difficult and it is rarely reported till now. There is no peaks indexed to carbon was observed for  $\text{Li}_2\text{MnSiO}_4/\text{C}$ , which may be attributed to the amorphous state of the residual carbon.



**Figure 1.** XRD pattern of the  $\text{Li}_2\text{MnSiO}_4/\text{C}$  sample.

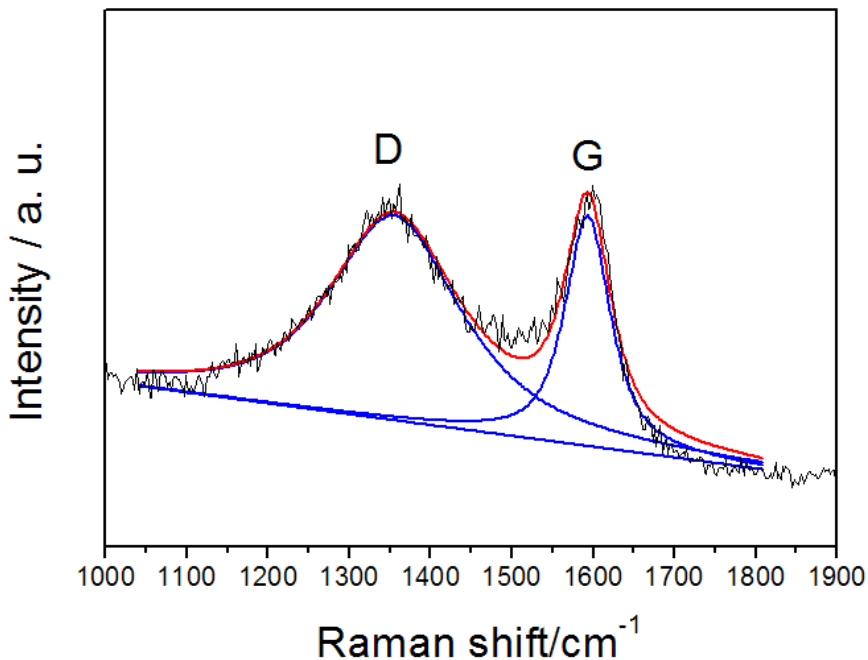
The morphological characteristics of  $\text{Li}_2\text{MnSiO}_4/\text{C}$  were investigated and the results were shown in Figure 2 (a)-(c). Small primary particles with the size of 50-80 nm were observed in the SEM image, which closely agglomerated together (Figure 2(a)). The presence of carbon layer on the surface

of nanoparticles was confirmed by TEM observation, which produces a carbon coating layer for the electrode material (Figure 2 (b)). The EDX mapping results of  $\text{Li}_2\text{MnSiO}_4/\text{C}$  are shown in Figure 3 (c), which exhibits uniformly distribution of the elements (C, Mn, Si) in the sample. The carbon content of the  $\text{Li}_2\text{MnSiO}_4/\text{C}$  sample was determined by TGA analysis and about 7 wt.% of residual carbon was detected in the sample.



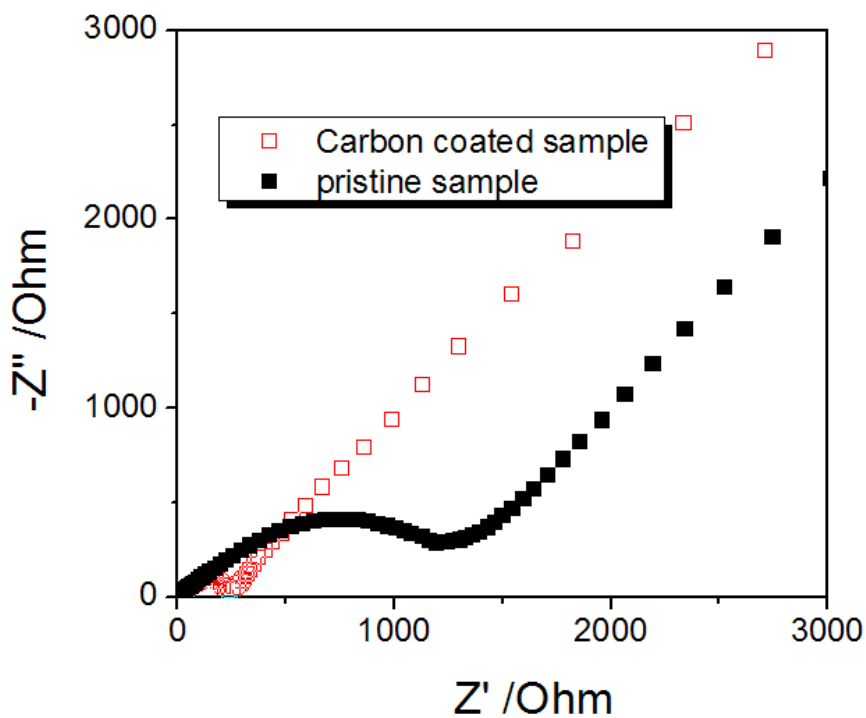
**Figure 2.** SEM (a), TEM (b) images and elements distribution mapping of C, Mn, Si (c) of the  $\text{Li}_2\text{MnSiO}_4/\text{C}$  sample.

Raman spectra analysis was employed to characterize the carbon phase. As shown in Figure 3, typical D and G bands of carbon appear around  $1350$  and  $1600\text{ cm}^{-1}$  respectively for the materials. The G-band originates from the in-plane bond-stretching motion of pairs of  $\text{sp}^2$  carbon atoms, while the D-band is associated with the  $\text{A}_{1g}$  symmetry, which is only active in the presence of disorder for  $\text{sp}^3$  carbon [20]. The peak intensity of the D and G bands ( $I_D/I_G$ ) generally provides a useful index for compare the degree of order of various carbon materials, i.e. a smaller ratio correspond to a higher degree of ordering in the carbon materials [21]. The calculated  $I_D/I_G$  ratios for  $\text{Li}_2\text{MnSiO}_4/\text{C}$  composites are 1.91. The result indicates low degree of ordering in the carbon material and the carbon phase is mainly amorphous for the samples, which is in agreement with above assumption.



**Figure 3.** Raman spectra of the  $\text{Li}_2\text{MnSiO}_4/\text{C}$  sample.

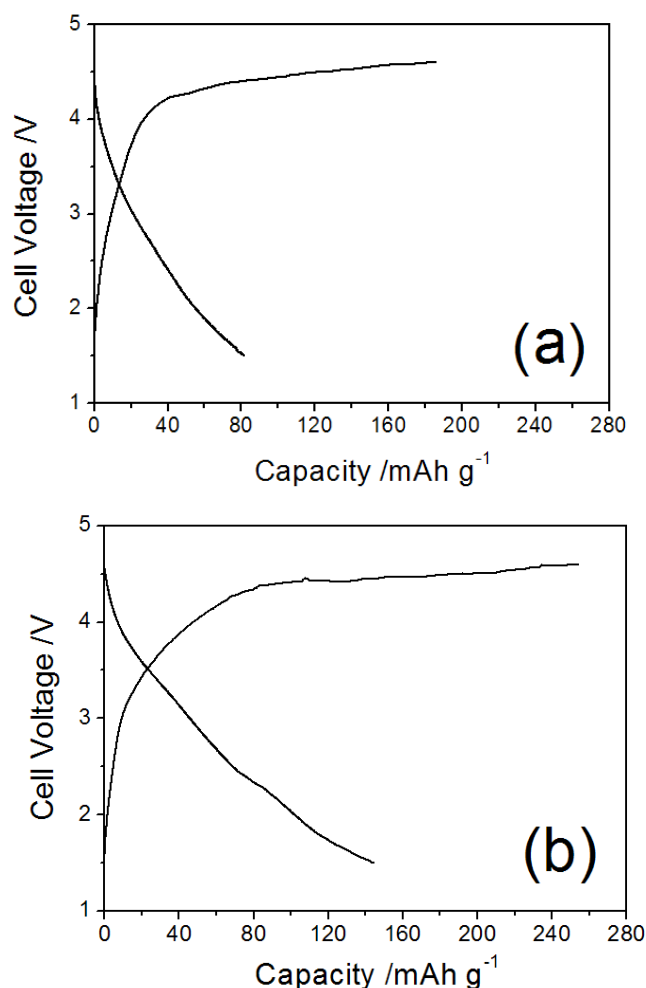
The electrochemical impedance spectroscopy of the pristine and carbon coated samples were compared in Figure 4.



**Figure 4.** Electrochemical impedance spectroscopy of the pristine  $\text{Li}_2\text{MnSiO}_4$  and carbon coated  $\text{Li}_2\text{MnSiO}_4/\text{C}$  samples.

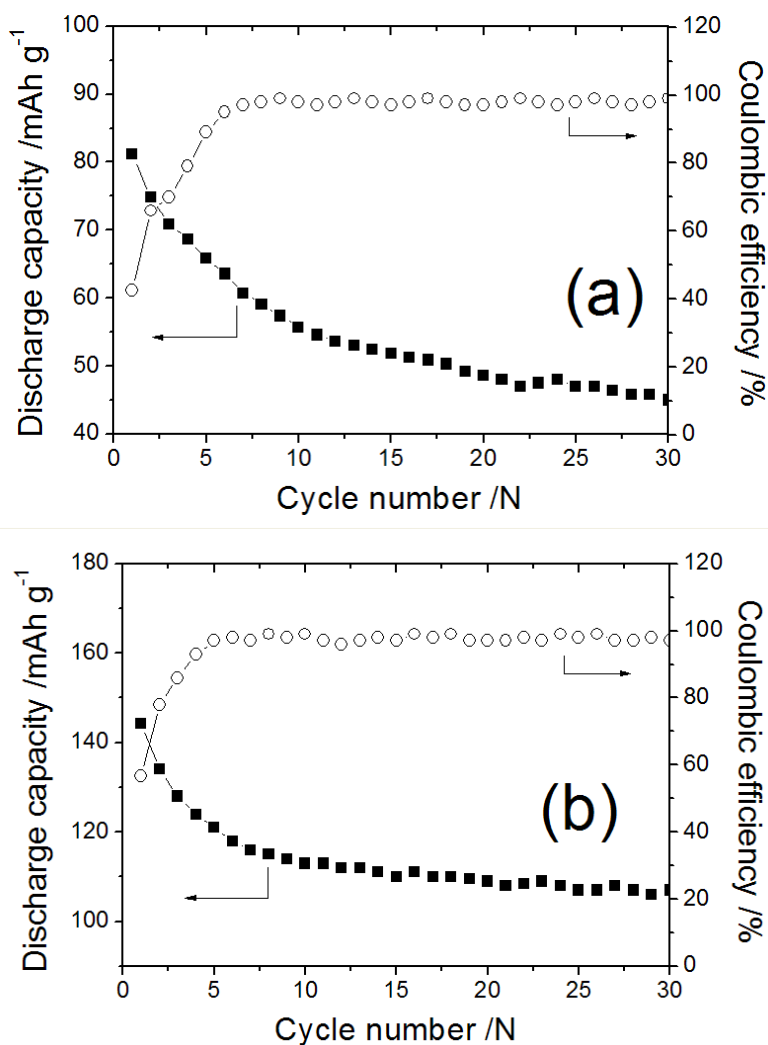
Each Nyquist plot consists of a depressed semicircle and a sloping line. The depressed semicircle and the sloping line can be respectively attributed to charge transfer reaction and solid-state diffusion of lithium ion. A larger semicircle is observed for the pristine sample ( $\text{Li}_2\text{MnSiO}_4$ ) than that of carbon coated one ( $\text{Li}_2\text{MnSiO}_4/\text{C}$ ), which indicates the higher charge transfer resistance of the pristine sample. The lower charge transfer resistance of  $\text{Li}_2\text{MnSiO}_4/\text{C}$  is associated with the thin carbon coating layer, which forms a high conductive layer on the particle surface and increases the conductivity of the electrode material. Therefore, the  $\text{Li}_2\text{MnSiO}_4/\text{C}$  sample exhibits improved electrochemical kinetic and enhanced electrochemical property is expected.

Figure 5 (a) and (b) compares the initial charge/discharge curves of the pristine and carbon coated samples. All the cells were assembled with lithium metal as the negative electrode and were tested in the voltage range of 1.5~4.6 V under a current density of  $10 \text{ mA}\cdot\text{g}^{-1}$ . Because of the low conductivity characteristics, poor electrochemical property and only about  $81 \text{ mAh}\cdot\text{g}^{-1}$  was obtained for the pristine sample in the initial discharge (Figure 5 (a)). For the carbon coated samples, the discharge capacity was improved and about  $144 \text{ mAh}\cdot\text{g}^{-1}$  was obtained in the initial discharge (Figure 5 (b)).



**Figure 5.** Initial charge/discharge curves of the pristine  $\text{Li}_2\text{MnSiO}_4$  (a) and carbon coated  $\text{Li}_2\text{MnSiO}_4/\text{C}$  (b) samples.

The discharge capacities and coulombic efficiencies of both samples were shown in Figure 6. In both cases, the low coulombic efficiencies were observed in the first cycle. As cycle number increases, the coulombic efficiencies were quickly improved and reached 99% after thirty cycles. However, this improvement was accompanied by a decrease of the capacity for both materials. After cycles, only about 58% and 75% of the initial discharge capacities were retained. A higher capacity retention of  $\text{Li}_2\text{MnSiO}_4/\text{C}$  is obtained compared with that of pristine one, which is also associated with its increased conductivity and improved electrochemical kinetic.



**Figure 6.** Discharge capacities and coulombic efficiencies of the pristine  $\text{Li}_2\text{MnSiO}_4$  (a) and carbon coated  $\text{Li}_2\text{MnSiO}_4/\text{C}$  (b) samples during cycling.

#### 4. CONCLUSIONS

$\text{Li}_2\text{MnSiO}_4/\text{C}$  with nanostructured particles and orthorhombic structure was synthesized via a modified sol-gel method. The particles of  $\text{Li}_2\text{MnSiO}_4/\text{C}$  with the size of about 80 nm were observed in the SEM image. A thin surface layer with amorphous carbon on nanoparticles was indicated by TEM

observation and Raman analysis. The carbon coated  $\text{Li}_2\text{MnSiO}_4/\text{C}$  exhibits improved charge/discharge capacities and cycling performance than the pristine one. The improvements are attributed to the decreased charge transfer resistance and enhanced conductivity induced by carbon coating.

#### ACKNOWLEDGEMENT

This work is supported by the Foundation for University Key Teachers by the Heilongjiang Ministry of Education (No. 1155G28).

#### References

1. A. R. Armstrong, N. Kuganathan, M. S. Islam, P. G. Bruce, *J. Am. Chem. Soc.*, 133 (2011) 13031.
2. S. Zhang, C. Deng, B. L. Fu, S. Y. Yang, L. Ma, *Electrochim. Acta*, 55 (2010) 8482.
3. A. Nyten, S. Kamali, L. Hanggstrom, T. Gustafsson, J. O. Thomas, *J. Mater. Chem.*, 16 (2006) 2266.
4. C. Deng, S. Zhang, Y. Gao, B. Wu, L. Ma, Y. H. Sun, B. L. Fu, Q. Wu, F. L. Liu, *Electrochim. Acta*, 56 (2011) 7327.
5. A. Nyten, A. Abouimrane, M. Armand, T. Gustafsson, J. O. Thomas, *Electrochem. Commun.*, 7 (2005) 156.
6. M. S. Islam, R. Dominko, C. Masquelier, C. Sirisopanaporn, A. R. Armstrong, P. G. Bruce, *J. Mater. Chem.*, 21 (2011) 9811.
7. Y. X. Li, Z. L. Gong, Y. Yang, *J. Power Sources*, 174 (2007) 528-532.
8. W. Liu, Y. Xu, R. Yang, *J. Alloy Compd.*, 480 (2009) L1.
9. R. Dominko, *J. Power Sources*, 184 (2008) 462.
10. V. Aravindan, K. Karthikeyan, K. S. Kang, W. S. Yoon, W. S. Kim, Y. S. Lee, *J. Mater. Chem.*, 21 (2011) 2470.
11. T. Muraliganth, K. R. Stroukoff, A. Manthiram, *Chem. Mater.*, 22 (2010) 5754.
12. C. Deng, S. Zhang, S. Y. Yang, B. L. Fu, L. Ma, *J. Power Sources*, 196 (2011) 386.
13. R. Dominko, M. Bele, A. Kokalj, M. Gaberscek, J. Jamnik, *J. Power Sources*, 174 (2007) 457-462.
14. C. Deng, S. Zhang, B. L. Fu, S. Y. Yang, L. Ma, *Mater. Chem. Phys.*, 120 (2010) 14.
15. S. Zhang, *Electrochim. Acta*, 52 (2007) 7337.
16. I. Belharouak, A. Abouimrane, K. Amine, *J. Phys. Chem. C*, 113 (2009) 20733.
17. V. Aravindan, K. Karthikeyan, J. W. Lee, S. Madhavi, Y. S. Lee, *J. Phys. D: Appl. Phys.*, 44 (2011) 152001.
18. P. Ghosh, S. Mahanty, R. N. Basu, *J. Electrochem. Soc.*, 156 (2009) A677.
19. V. Aravindan, K. Karthikeyan, S. Ravi, S. Amaresh, W. S. Kim, Y. S. Lee, *J. Mater. Chem.*, 20 (2010) 7340.
20. J. F. Qian, M. Zhou, Y. Cao, X. P. Ai, H. X. Yang, *J. Phys. Chem. C*, 114 (2010) 3477.
21. E. Markevich, R. Sharabi, O. Haik, V. Borgel, G. Salitra, D. Aurbach, G. Semrau, M. A. Schmidt, N. Schall, C. Stinner, *J. Power Sources*, 196 (2011) 6344.